Carbon Nanotube Silicon Heterojunction Solar Cells

LePing Yu, Daniel Tune and Joe Shapter

School of Chemical and Physical Sciences, Sturt Road, Bedford Park, South Australia, 5042, AUSTRALIA, leping.yu@flinders.edu.au; daniel.tune@flinders.edu.au; joe.shapter@flinders.edu.au

ABSTRACT

The use of polymers within silicon-carbon nanotube heterojunction photovoltaics has been explored. Nanocomposites involving the carbon nanotubes as well as various layered structures have been used. A thin conducting polymer interlayer significantly improves photovoltaic performance by creating a better depletion layer within the underlying silicon while other polymers can be used as effective antireflection layers. Mixtures of CNTs and polymers can also improve performance. With a combination of these approaches a photovoltaic device has been fabricated with a photovoltaic conversion efficiency of 8.7 %.

Keywords: SWCNTs, solar cells, conductive polymers, nanocomposite, anti reflection layers.

1 INTRODUCTION

In order to overcome some of the production costs of conventional silicon-based solar cells, as well as to counter the toxicity and/or scarcity of some alternatives including indium, cadmium, ruthenium and lead, researchers have made great efforts in the last a few decades to pioneer the use of carbon materials as components of light harvesting devices [1]. One such material is carbon nanotubes (CNTs) which have shown excellent electronic and optical properties since their discovery in 1991[2]. Si-CNT heterojunction solar cells are an alternative to conventional silicon devices, where the cost-intensive fabrication of a p-type silicon layer is replaced by deposition of a highly transparent CNT film [3]. The transparent film allows many incident photons to reach the silicon and be absorbed to create electron-hole pairs. Following exciton diffusion to the depletion region, created by the interaction of the p-type nanotubes and n-type silicon, dissociation occurs under the influence of the built-in potential resulting from equilibration of the silicon and CNT Fermi levels, with the holes and electrons acting as the majority charge carriers in the CNT and silicon layers, respectively [4].

Polymers form another class of carbon-based materials which have also been studied as materials for solar cells using simple fabrication process [5]. So far, major efforts have been made in both Si-CNT and Si-organic solar cells separately [6]. For example, with the introduction of titanium dioxide as an antireflection layer, and following doping of the CNT film with HNO_3 and H_2O_2, a Si-CNT device with an efficiency of 15 % has been fabricated [7].

2 MATERIALS AND METHOD

CNT stock solution (0.1 mg mL^{-1}) was prepared by dispersing arc-discharge cnt powder (P3-SWNT, Carbon Solutions inc., USA) in aqueous Triton x-100 (1 % v/v, Sigma-Aldrich, Australia) by bath sonication (S 30H, Elmasonic) for 1 h at room temperature. The resulting CNT suspension was centrifuged at 17 500 × g for 60 min (Allegra x-22 centrifuge, Beckman Coulter). The supernatants from all six centrifuge tubes were collected, combined, and then centrifuged again in the same manner as previously, with the bottom residue being discarded. The supernatants from this second centrifuge cycle were then collected and combined to yield the stock solution [8].

Polymer layers were deposited from dilute solutions of commercial polymer materials. For the antireflection polyerms, a mixture of PDMS prepolymer and curing agent (10:1; weight ratio, Sylgard 184, Dow Corning, Midland, MI) was stirred and mixed completely and degassed under vacuum. The PMMA solution was prepared by dissolving solid PMMA (M_w: 120 000, Sigma-Aldrich, Australia) in acetone with the concentration of 2.2 wt%. PS solutions were prepared by dissolving PS (M_w: 230 000, Sigma-Aldrich, Australia) in toluene with the concentration of 1.85 wt%, 2.2 wt% and 2.85 wt%.

For PANI, an emeraldine salt solution was prepared by dissolving emeraldine base (M_w: 10 000, Sigma-Aldrich, Australia) in acetic acid (80 % v/v) at a concentration of 0.58 mg mL^{-1}. The P3HT solution was prepared by dissolving P3HT solid (M_w: 63 000, Sigma-Aldrich, Australia) in toluene at a concentration of 0.45 mg mL^{-1}. PEDOT:PSS suspension was diluted 10 times from stock (Clevios PVPAI 4083) and its concentration was 1.5 mg mL^{-1}. All conducting polymer solutions were passed through Teflon filters (0.45 µm) to remove large particles in order to reduce defects during film formation. PS solutions were prepared by dissolving PS (M_w: 230 000, Sigma-Aldrich, Australia) in toluene at 2.2 wt%.

Various volumes of CNT suspension were diluted in 250 mL aqueous TritonX-100 (0.01 % v/v) to achieve CNT films with 70 % transmittance. The diluted CNT suspension was then filtered onto a target mixed cellulose ester (MCE) membrane (0.45 µm, HAWP, Millipore, Australia) with the assistance of a nitrocellulose 'stencil' membrane with 4 × 0.49 cm^2 holes (25 nm, VSWP, Millipore, Australia). The difference between pore sizes of the two membranes enables fast flow rate at through the four cut-out areas and four identical CNT membranes could be collected in one filtering. Then, CNT films were rinsed with 3 X 50 mL

water followed by a further 250 mL of water in order to remove any remaining surfactant. For device fabrication, a central circular area (0.32 cm^2) was cut out from each membrane.

Phosphorous doped n-type silicon wafers (5-10 Ω cm, 525 µm thick with a 100 nm thermal oxide, ABC GmbH, Germany) were used as substrates for the devices. Positive photoresist (AZ1518, micro resist technology GmbH, Munich, Germany) was applied by spin coater (3000 rpm, 30 s) on the Si and soft-baked at 100 °C for 60 s. A mask was put on this resist and UV photolithography defined an active area (0.079 cm^2), which was developed by developer (AZ 326 MIF, AZ electronic Materials, GmbH, Munich, Germany) and Ti/Au (5/145 nm/nm) was sputtered (with deposition controlled by quartz crystal microbalance, Quorumtech K757X) as the front metal contact. Then, the photoresist was lifted off by immersion in acetone for 30 min. One drop of buffer oxide etch (BOE, 6:1 of 40% NH_4F and 49% hydrofluoric acid (HF), Sigma-Aldrich, Australia) was used to etch the front 100 nm thermal oxide layer. The circular CNT/MCE films were placed on top of the substrates (CNT side down). A drop of water was used to wet the film and the device was then baked at 80 °C for 15 min. After cooling, the substrate with CNT/MCE was immersed in 3 sequential baths of clean acetone (30 min each) to dissolve the MCE. Following scratching of the back oxide layer of silicon, a gallium indium eutectic (eGaIn) was used to mount cells onto stainless steel plates (Figure 1). The resulting cells are 'as prepared' devices.

There are three post treatments for these films. Firstly, a droplet of HF (2 %) was applied on the active area for 10 s, followed by rinsing of the cell surface with water, ethanol and drying with nitrogen gas in order to etch away the silicon oxide layer formed during the device fabrication. Instead of HF, hydrochloric acid (2 %) was applied in the same manner on the glass slides to avoid the reaction between the glass and HF. Secondly, a drop of $SOCl_2$ was added onto the PANI/CNT or pure CNT surfaces to improve the conductivity of the membrane by shifting the Fermi level of the CNT to the valence band and also reducing the junction resistances between CNTs [9]. Thirdly, a second HF treatment was done in the same manner as the first one to remove the silicon oxide layer formed during the $SOCl_2$ treatment.

The performance of the devices (current density versus voltage curves, J-V) was evaluated by a custom Labview™ virtual instrument with a Keithley 2400 source unit. By using a standard cell (PV Measurements, NIST-traceable certification), the power density of the collimated Xenon-arc light at the cell surface was calibrated to 100 mW cm^{-2} with the light passing through an AM 1.5G filter. Both the light and the dark curves were measured to determine the performance and the diode properties of the devices. The diode properties were evaluated by fitting the dark current data to the following equation: $J = J_{sat} [e^{(qv)/(nkt)} - 1]$ (J_{sat}: reverse saturation current, q: elemental charge, V: applied voltage, n: ideality, k: Boltzmann constant, T: temperature) [10]. The sheet resistance of the films was evaluated using a four point probe in linear configuration (Keithlink).

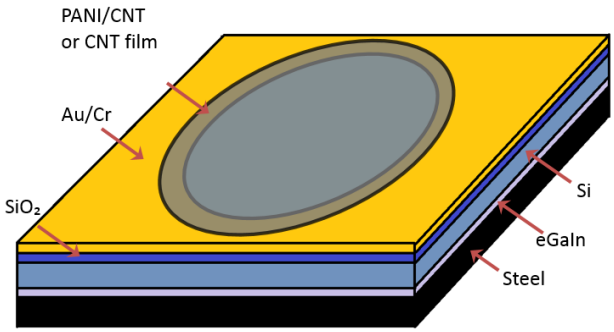

Figure 1. Schematic showing the general structure of the CNT-Si solar cells

3 RESULTS

Figure 2 shows the current density-voltage (J-V) curves measurements of devices involving conducting polymer interlayers. The polymer-only devices have very poor performance in all respects, including low short circuit current density (J_{sc}), open circuit voltage (V_{oc}), fill factor (FF), and power conversion efficiency (PCE) along with high ideality and reverse saturation current density (J_{sat}). This is because the thin conducting polymer layer has limited ampacity, especially P3HT. Si-CNT devices show much better performance compared to Si-CP devices because the CNT film has a lower sheet resistance ($R_{sheet} \approx 400\ \Omega\ square^{-1}$) and higher ampacity than the conducting polymer layers ($R_{sheet} > 10^6\ \Omega\ square^{-1}$). The PCE of the Si-CNT control device is normally around 5 % [3l]. After addition of PANI, P3HT or PEDOT:PSS between the silicon substrate and the CNT films, both J_{sc} and V_{oc} are improved compared to devices without the polymer. Additionally, there is a significant increase in FF, especially after adding the PEDOT:PSS interlayer. The conducting polymer modified devices also have better ideality and 1-2 orders of magnitude lower J_{sat} compared to the devices without the polymer. These improvements indicate that a better depletion region is formed in the silicon, meaning that electron-hole pairs can be separated more effectively. This is likely a result of the PANI, P3HT and PEDOT:PSS layers forming a conformal covering on the silicon surface whereas sparse CNT networks limit the overall photoactive junction interfacial area due to a smaller area with intimate contact between the p-type and n-type material [8]. After introducing a conducting polymer interlayer between silicon and CNT film, there is a larger intimate contact area on silicon compared to CNT film. Thus, the ability to collect charge carriers in the Si-CNT device is worse than that of Si-PANI-CNT, Si-P3HT-CNT and Si-PEDOT:PSS-CNT cells. As shown in Figure 2 (d), all three conducting polymer modified Si-CNT solar cells have similar V_{oc} with

slight differences in J_{sc}. However, the FF of the Si-PEDOT:PSS-CNT device is 0.11 - 0.14 higher than that of the other two devices. For this reason, the Si-PEDOT:PSS-CNT has the highest PCE (7.7 %) among the three.

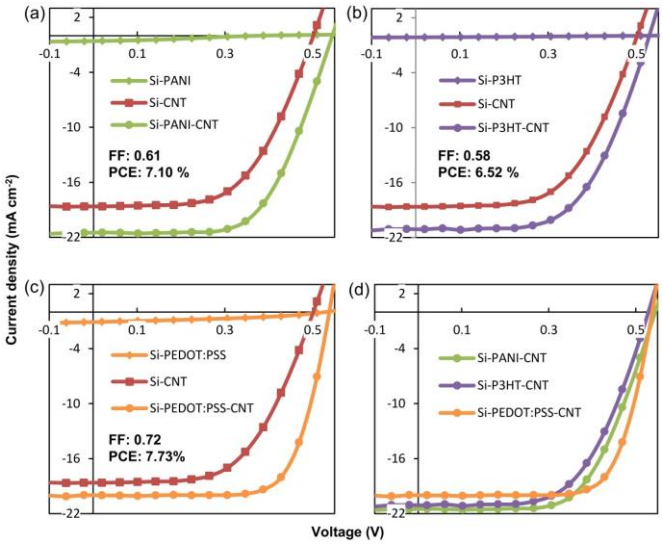

Figure 2. Current density-voltage measurements of solar cells with (a) PANI, (b) P3HT and (c) PEDOT:PSS. Each plot shows the light curves obtained from Si-CP, Si-CNT and Si-CP-CNT devices and (d) shows a comparison between Si-PANI-CNT, Si-P3HT-CNT and Si-PEDOT:PSS-CNT.

As shown in Figure 3 (a), the reflectance of silicon surface with a CNT film is very high (about 30 % over a wide wavelength range from about 550 to 1050 nm where silicon can absorb energy from the incident light). Since the transmittance of all 3 types of he AR polymers is very close to 100 % over the wavelength where silicon can efficiently produce excitons, the decreased reflectance is due to the antireflection function of polymer layers [7,11,12]. The PDMS film had the worst antireflection effect of all three polymers. The PMMA coated surface had its lowest reflectance near 800 nm. The particular PS layer in Figure 3 (a) exhibited a comparatively low reflectance over the whole active range of silicon. Figure 3 (b) shows the impact of antireflection polymer layers on the performance of Si-CNT devices. Clearly, adding an antireflection layer improved the performance but the three polymers showed different levels of effectiveness. The absolute increases of the PCE by adding PDMS, PMMA and PS were 0.24 % (6.17 – 5.93 %), 0.56 % (6.54 – 5.98 %) and 0.79 % (7.10 – 6.31%), respectively. The difference of improvement is related to the antireflection effect of different polymers whereby a lower reflectance means a greater improvement in cell efficiency. In Figure 3 (a), the PS coated surface has the least reflectance and the PDMS coated surface has the highest reflectance, which is consistent with the changes in PCE after coating.

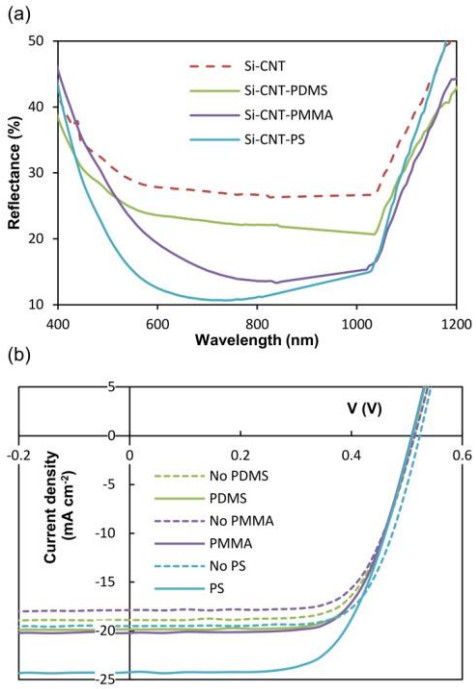

Figure 3. (a) Reflectance spectra of Si-CNT surfaces with various polymers (PDMS, PMMA and PS); the three films have different thicknesses. (b) Representative J-V curves of Si-CNT devices before and after adding various antireflection coatings (PDMS, PMMA and PS) with different thickness. Solid/dashed curves represent devices after the second HF treatment with/without antireflection polymer layers.

Given that the PEDOT:PSS interlayer cells gave the best performance, further efforts to improve this performance were undertaken. As discussed earlier, adding an antireflection layer such as PDMS or PMMA has been shown to increase the performance of Si-CNT devices by helping the silicon surface to trap more energy from the incident light [11,13]. Here, PS, has been used for the same purpose to build Si-PEDOT:PSS-CNT-PS cell. The influence of a series of treatments applied to the devices post-fabrication (but before PS addition) is shown in Figure 4. The as-prepared, untreated device has limited performance as was the case for the Si-CNT devices, including a high series resistance and low shunt resistance, J_{sc}, FF and PCE. This could be due to the fact that HF has a light doping effect via protonation of the PEDOT in the PEDOT:PSS interlayer. As a result, the ability to maintain separation of electron-hole pairs has been improved and the cell has a higher FF (0.46) compared to that of a similarly treated Si-CNT device. However, after $SOCl_2$ treatment the performance decreases in the same manner as for Si-CNT devices. After a second HF treatment, the performance of the Si-PEDOT:PSS-CNT device is improved again due to a slight increase of J_{sc}, V_{oc} and a dramatic increase of the FF, from 0.28 to 0.72. As shown in Figure 4 after adding the PS antireflection layer there is a clear improvement of J_{sc} and

the PCE is increased to 8.7 % due to increased incident light absorption by the silicon because of the reduced reflectance of the surface.

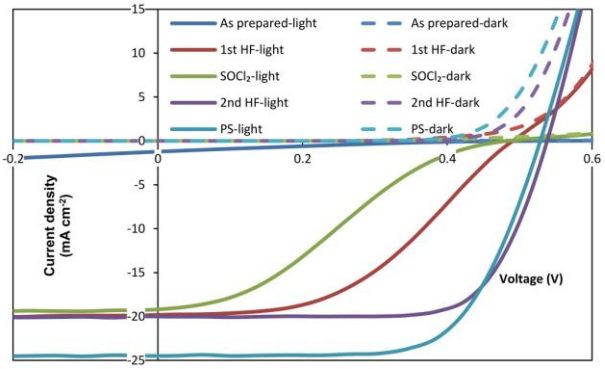

Figure 4. Light and dark current density -voltage measurements (solid lines: light curves; dashed lines: dark curves) of device with 4-layer structure Si-PEDOT:PSS-CNT-PS (after all post treatments (HF-$SOCl_2$-HF) and adding PS antireflection layer).

There are few studies regarding the application of conducting polymer/carbon nanotube composite electrodes in CNT-Si heterojunction solar cells. To further investigate this design, and in contrast with previous work in which the polymer was applied on top of or underneath the nanotubes, we prepared the PANI/CNT composites by premixing CNTs and PANI in solution followed by vacuum filtration as it was expected that this would improve the quality of the interface through providing more intimate contact over greater areas.

It was shown that the addition of the conducting polymer into the nanotube film significantly improved the electrical conductivity and thus the performance of the solar cells (see Figure 5). The effects of different constituent ratios were also explored and the performance of the solar cells was increased significantly by optimising the film composition. This was shown to be due to a balance between minimising the films' sheet resistance whilst maximising their electrical to optical conductivity ratio, as well as the absolute amount of incident light penetrating through to the underlying silicon.

4 CONCLUSIONS

The results of this study show conclusively that in terms of overall photovoltaic output, the nanoscale morphology at the interface, which controls the quality of the heterojunction, is a pivotal characteristic over and above any optimisation of the electrical/optical properties of the contacting electrode.

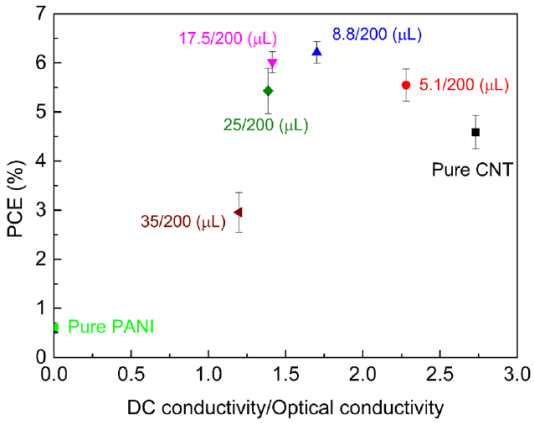

Figure 5. PCE versus DC/OP conductivity of films with different material ratios (PANI/CNT).

REFERENCES

[1] D. D. Tune, B. S. Flavel, R. Krupke, J. G. Shapter, *Adv. Energy Mater.* 2012, *2*, 1043-1055.

[2] S. J. Wang, M. Khafizov, X. M. Tu, M. Zheng, T. D. Krauss, *Nano Lett.* 2010, *10*, 2381-2386.

[3] D. D. Tune, F. Hennrich, S. Dehm, M. F. G. Klein, K. Glaser, A. Colsmann, J. G. Shapter, U. Lemmer, M. M. Kappes, R. Krupke, B. S. Flavel, *Adv. Energy Mater.* 2013, *3*, 1091-1097.

[4] Y. Jia, A. Y. Cao, X. Bai, Z. Li, L. H. Zhang, N. Guo, J. Q. Wei, K. L. Wang, H. W. Zhu, D. H. Wu, P. M. Ajayan, *Nano Lett.* 2011, *11*, 1901-1905

[5] G. Li, R. Zhu, Y. Yang, *Nat. Photonics* 2012, *6*, 153-161.

[6] R. Liu, S. T. Lee, B. Sun, *Adv Mater* 2014, *26*, 6007-6012.

[7] E. Z. Shi, L. H. Zhang, Z. Li, P. X. Li, Y. Y. Shang, Y. Jia, J. Q. Wei, K. L. Wang, H. W. Zhu, D. H. Wu, S. Zhang, A. Y. Cao, *Scienitific Reports* 2012, *2*, 884.

[8] D. D. Tune, B. S. Flavel, J. S. Quinton, A. V. Ellis, and J. G. Shapter, *Chemsuschem* 2013, *6*, 320-327.

[9] Y. Jia, A. Y. Cao, X. Bai, Z. Li, L. H. Zhang, N. Guo, *et al.*, *Nano Letters* 2011, *11*, 1901-1905.

[10] S. K. Cheung and N. W. Cheung, *Applied Physics Letters I 49*, 85-87.

[11] R. Li, J. Di, Z. Yong, B. Sun, Q. Li, *J. Mater. Chem.* 2014, *2*, 4140-4143.

[12] X. Li, X. H. Yu, Y. C. Han, 2013. *J. Mater. Chem. C* 2013, *1*, 2266-2285.

[13] Y. Jia, P. Li, X. Gui, J. Wei, K. Wang, H. Zhu, D. Wu, L. Zhang, A. Cao, Y. Xu, *Appl. Phys. Lett.* 2011, *98*, 133115